J Mater Sci (2007) 42:6446–6452
DOI 10.1007/s10853-006-1227-9

Spatial distribution of pores in lotus-type porous metal

Jiang Wan · Yanxiang Li · Yuan Liu

Received: 14 June 2006 / Accepted: 6 November 2006 / Published online: 25 April 2007

Abstract The spatial distribution of pores in lotus-type porous magnesium has been studied with the second-order characteristics and the nearest-neighbour distance distribution by using statistical analysis methods. The results show that the spatial distribution of pores is short-range ordered. On the basis of the analysis, two structural indices deduced from the variance of nearest-neighbour distance distribution and the standard deviation of local porosity from Dirichlet tessellations were proposed for quantitatively characterizing the pore distribution.

Introduction

Porous and foamed metallic materials have become an attractive research field both from a scientific viewpoint and the prospect of industrial applications because of their unusual combinations of many physical and mechanical properties. Recently, a new type of porous metal with long cylindrical pores aligned parallel to the solidification direction has been fabricated by the metal/gas eutectic unidirectional solidification method (also called ''Gasar'' process) [1]. This processing technique utilizes an invariant reaction of 'metal/gas eutectic reaction' in which the melt is solidified into a solid solution and a gas phase. Compared with traditional fabrication techniques, this process allows an effective control of porosity and pore morphology. The formed porous structure is designated as lotus-type because it looks like lotus root. It was found that the lotus-type porous metals exhibit superior mechanical properties than conventional porous metals. Thus they are expected to have many potential applications [2–4]. Size, shape and distribution of pores are the most essential and important characteristics of porous materials. Characteristics of the lotus-type structure include bulk porosity, pore diameter and spatial distribution of pores. Bulk porosity and pore size have been studied theoretically and experimentally [5–9], but study of spatial distribution of pores is lacked. There has been no quantitative characterization of the spatial distribution of pores in the literatures yet. For the purpose of a thorough understanding of the microstructure-property relationships and accurately modeling and predicting the properties of lotus-type porous metals, it is necessary to quantitatively describe the spatial distribution of pores and measuring the degree of non-uniformity.

Lotus-type porous metals can be considered as a two-phase material. The pores, as the second phase, separately distribute in metal matrix. There have been a lot of methods for the quantitative characterization of the second-phase distribution [10–14]. The fluctuations of microstructures are often described by the so-called second-order characteristics. The second-order analysis of point patterns has been used in studies of particle and fibre distribution in composite materials. Generally functions such as second-order intensity function, pair correlation function and so on are used as informative descriptors of the point (or second-phase centroids) distribution. In the case when the investigation of the second-order analysis does not give conclusive results, it is

J. Wan · Y. X. Li · Y. Liu
Key Laboratory for Advanced Materials Processing Technology, Ministry of Education, Beijing 100084, P.R. China

J. Wan · Y. X. Li (✉) · Y. Liu
Department of Mechanical Engineering, Tsinghua University, Beijing 100084, P.R. China
e-mail: yanxiang@tsinghua.edu.cn

necessary to invoke other pattern discriminators, which are based upon the Dirichlet cell properties or inter-point statistics such as nearest-neighbour distance [10]. Dirichlet tessellation is the subdivision of a region, determined by the centroids of the second phase. It is capable of revealing spatial relationships of pores on a transverse cross-section. Nearest neighbour distance distribution is as well an effective means to quantify and discriminate different point patterns by describing inter-point relationships.

In this paper, the spatial distribution of pores in lotus-type porous magnesium fabricated at various gas pressures is analyzed with the above-mentioned methods. Since there exists a quasi-steady stage in the Gasar process and the separated pores are nearly parallel in the solidification direction [8–9], the pore distribution on a transverse cross-section is representative for the spatial distribution of pores in the steady-state region of ingots. By investigating the distribution of pore centroids on a transverse cross-section, pore distributions are extensively described either qualitatively or quantitatively. It was found that the nearest-neighbour distance of pore centroids and the ratio of the cross-sectional area of the pore to the corresponding Dirichlet polygon area are sensitive to the pore distribution of lotus-type structure in contrast with other parameters. Two quantitative indices for pore distribution are proposed subsequently.

Experimental procedure

Samples

A schematic of the fabrication apparatus for lotus-type porous metals is shown in Fig. 1. The specimens were fabricated as follows: high-purity 99.99% magnesium was melted in the crucible under an atmosphere of high-pressure hydrogen or gas mixture of hydrogen and argon; the melt was held superheated at a constant temperature until the dissolved hydrogen reached its saturation, then poured into a cylindrical mould with a water-cooled copper chiller at the bottom base. Thus the melt was solidified unidirectionally upwards. Straight pores were formed by the supersaturated hydrogen precipitated in solidification. The ingots obtained were 75 mm in diameter and 70–120 mm in height dependent upon the porosity. The observed transverse cross-sections were cut at 1/2 height of the ingots by electro-discharge machining. Table 1 lists the bulk porosity ($\bar{\varepsilon}$) of ingots and mean diameter of pores ($\bar{D}$) on the observed section areas produced at different combinations of hydrogen and argon pressure.

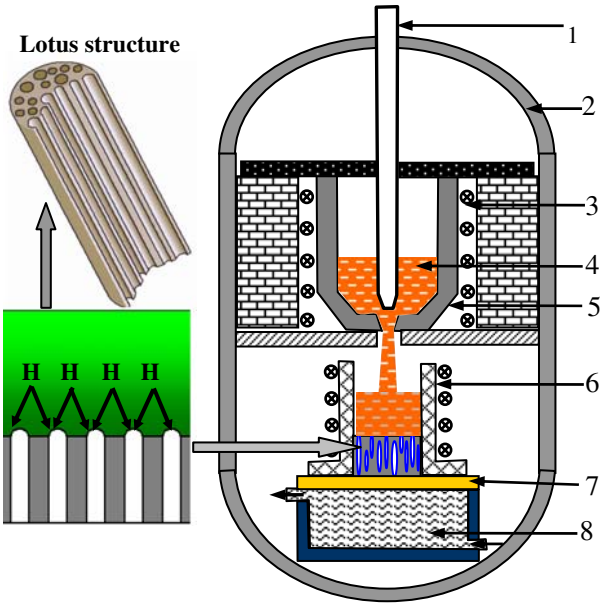

Fig. 1 A schematic of the fabrication apparatus for lotus-type porous metals: (1) graphite stopper; (2) high pressure chamber; (3) heating coil; (4) molten metal; (5) graphite crucible; (6) ceramic mould; (7) copper chiller; (8) cooling water

Table 1 The bulk porosity of ingots and mean diameter of pores produced at different gas pressures (Holding temperature T = 1023 K)

Sample No.	1	2	3	4	5	6	7
P_{H_2} (MPa)	0.2	0.4	0.7	1.0	0.4	0.4	0.4
P_{Ar} (MPa)	0	0	0	0	0.2	0.4	0.6
$\bar{\varepsilon}$	0.43	0.37	0.30	0.28	0.31	0.24	0.20
$\bar{D}$ (mm)	0.58	0.32	0.22	0.18	0.26	0.24	0.28

Methods of measurement

In lotus-type porous metals, separated pores are almost parallel in the solidification direction. Therefore a parallel bundle of straight non-intersecting tubes model is suitable to describe the special 3-D pore structure. During the Gasar process, there exists a quasi steady-state solidification condition [8–9]. There is only a little fluctuation of pore structure along the height in the steady-state stage; while large fluctuations of pore structure appear in the unsteady-state stage at the initiation and end of solidification, which was not taken into account in this paper. Thus the pore distribution on a typical transverse cross-section was used to approximate the spatial distribution of pores formed under steady-state solidification condition. Images of the cross-sections were processed by an image analysis system

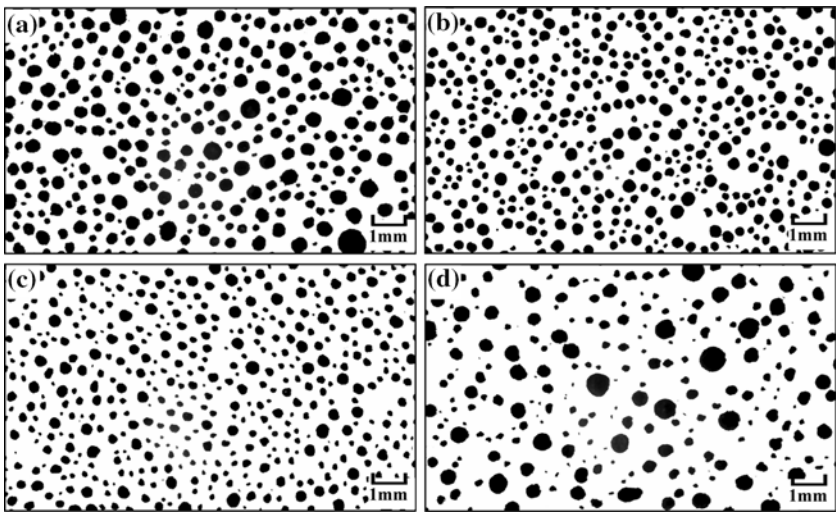

Fig. 2 Distribution of pores on transverse cross-sections of lotus-type porous magnesium, (**a**) sample No.2; (**b**) sample No.3; (**c**) sample No.5; (**d**) sample No.7

with which the coordinates of the centroid and the diameter of each pore were recorded. Some of the images are shown in Fig. 2.

The second-order characteristics of pore distribution were studied with the second-order intensity function $K(r)$ and the pair correlation function $g(r)$ that describe the variation and correlation in point fields. Theoretical backgrounds of the two functions have been discussed in [15]. For the completely random Poisson distribution, $K(r) = \pi r^2$ and$g(r) \equiv 1$. The $K(r)$ function for the completely random Poisson distribution usually serves as a dividing line between clustered point patterns and patterns with a certain degree of regularity [10]. The estimated curve for $K(r)$ falling below that for $K(r) = \pi r^2$ implies that the point pattern exhibits regularity, whereas the curve lying above implies a clustered point pattern.

The nearest-neighbour distance distribution is estimated by measuring the nearest distance between centroids of neighbouring pores. A proposed method for distinguishing random, clustered and regular point patterns relies on comparison of the mean nearest-neighbour distance as well as the variance, with the values for a random distribution [11]. The mean nearest neighbour distance $E(r)$ for a random distribution of points is given by

$$E(r) = \frac{0.5}{\sqrt{\lambda}} \tag{1}$$

and the variance $E(s^2)$ is given by

$$E(s^2) = \frac{4-\pi}{\pi} \cdot \frac{1}{\lambda} \tag{2}$$

where λ is the point density which indicates the point number per unit area on a planar area. For a given point density, based on the ratio (Q) of the measured mean nearest-neighbour distance to the one for random distribution and the ratio (R) of the measured variance to the one for random distribution, it is possible to distinguish between random sets (Q~1, R~1), short-range ordered sets ($Q > 1$, $R < 1$), clustered sets ($Q < 1$, $R < 1$), and sets of clusters with a superimposed background of random points ($Q < 1$, $R > 1$) [11]. The degree of the deviation from ideal regularity of point sets can be quantitatively described by the ratio R. For ideal regularity, R equals to 0. The larger the ratio R, the lower is the regularity.

The Dirichlet tessellation generated by the centroids of pores as shown in Fig. 3 would be the final method in determining the pore distribution [12–14]. Each Dirichlet polygon contains only one corresponding pore. Generally we assume the distribution of uniform pores is in a uniform hexagonal array on a plane for ideal lotus-type structure, i.e. the Dirichlet polygons (or the pore-cells) are uniform hexagons, whereas the actual pore-cells deviate greatly from the ideal ones in the pore size and cell shapes. Measuring the area of individual polygons by computer, the local porosity of each cell is calculated from

$$\varepsilon_c = S_p/S_c \tag{3}$$

where ε_c is the local porosity in a pore-cell, S_p and S_c are the areas of the pore and its corresponding polygon respectively. The standard deviation of the local porosity distribution is a measure of the degree of uniformity of the pore-cells, which indirectly represents the characteristics of pore distribution. The lower the standard deviation, the more uniform are the pore-cells.

In order to minimize the edge error in calculations, a rectangular measuring area is chosen at the center of each original image and all pores, which the Dirichlet polygons are not completely contained in the measuring area are

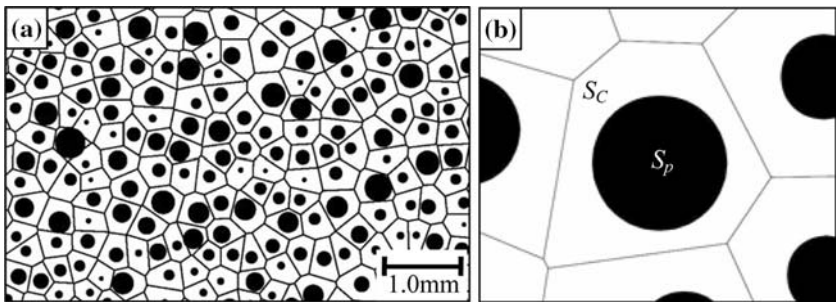

Fig. 3 Dirichlet tessellation for a transverse cross-section, (**a**) the Dirichlet tessellation of sample No.5; (**b**) the definition of local porosity

deleted in the calculation of inter-pore distances. Increasing the size of the analyzed area would also decrease the edge error. In the present study, the size of the measuring area is 40×20 mm^2, usually containing a number of pores about 2,000 or more.

Results

Second-order characteristics

The second-order intensity functions $K(r)$ for centroids of pores on transverse cross-sections are shown in Fig. 4. In a short range of r, all the estimated curves for $K(r)$ functions of lotus-type porous magnesium specimens are beneath that for the random distribution.

The pair correlation functions $g(r)$ for the specimens are shown in Fig. 5, which is the typical form for that of a point field with weak short-range order [15]. It was found that there is an inhibition distance during which the $g(r)$ keeps zero. The maximums and minimums are related with the degree of uniformity in the pore distribution. Finally, beyond a distance of about 2–3 times mean pore diameter, $g(r)$ functions tend to unity, which indicates the randomness of pore distribution at a larger range. In Fig. 5 clear peaks exist in most of the function curves, showing regularity of the distribution in the corresponding range. However for specimens fabricated at higher argon pressures, the maximums and minimums are obviously not as sharp as that for the other $g(r)$ functions, as shown in Fig. 5b.

Nearest-neighbour distance distribution

The nearest-neighbour distance distribution of pore centroids for several specimens is shown in Fig. 6. For corre-

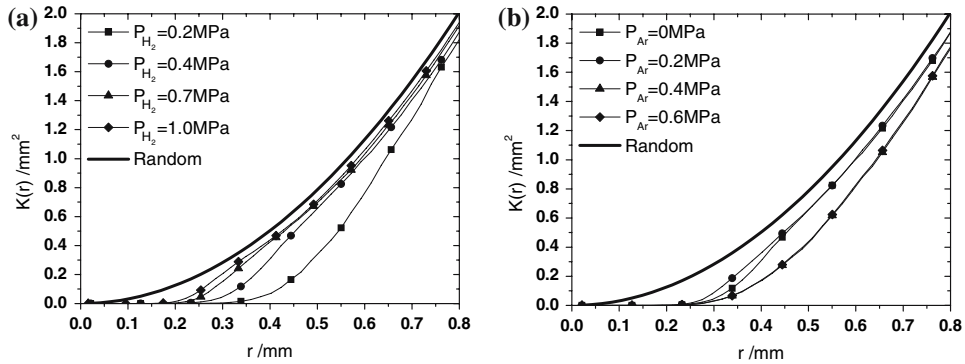

Fig. 4 Second-order intensity function for lotus-type porous magnesium, (**a**) pure hydrogen; (**b**) constant $P_{H_2} = 0.4$ MPa

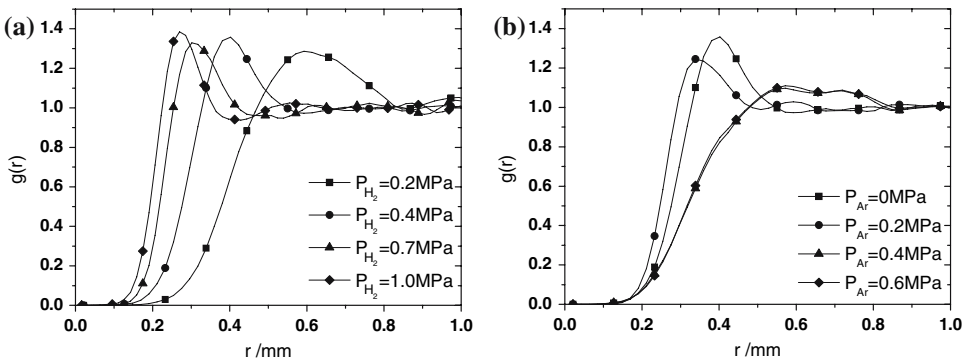

Fig. 5 Pair correlation function for lotus-type porous magnesium, (**a**) pure hydrogen; (**b**) constant $P_{H_2} = 0.4$ MPa

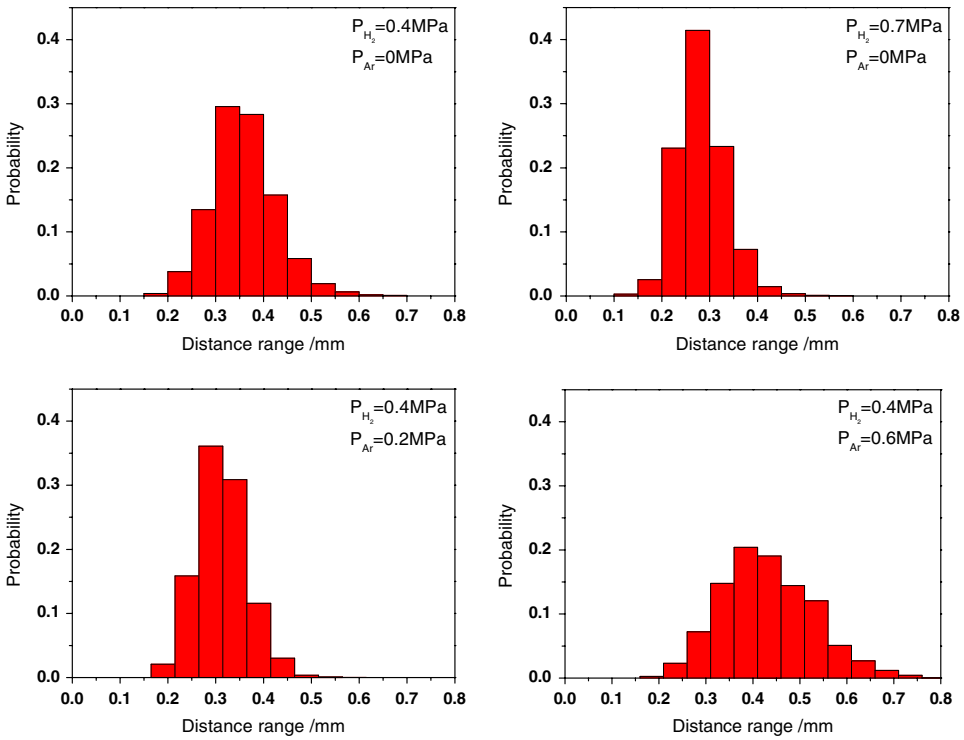

Fig. 6 Nearest-neighbour distance distribution of pores on transverse cross-sections

sponding ratio Q and R listed in Table 2, there are $Q > 1$ and $R < 1$, indicating that the pore distribution is short-range ordered. The relationship between the fabrication parameter—gas pressure and the ratio R describing distribution regularity is shown in Fig. 7. At a pure hydrogen atmosphere, the regularity increases with the hydrogen pressure; while at a constant hydrogen pressure plus additional argon, the regularity first increases with the argon pressure, then decreases. These indicate that at a certain hydrogen pressure, there is an optimized argon pressure corresponding to the highest regularity. The ratio Q provides some information about distribution types. For the square and regular hexagonal array which are commonly assumed in modeling, $Q = 2$ and $Q = 2.15$, respectively. However, ratios Q for the examined specimens are round 1.5, greatly different from those of both structures above.

Local porosity distribution

The local porosity distribution of several specimens is shown in Fig. 8. The relationship between gas pressure and the standard deviation is shown in Fig. 9. At a pure hydrogen atmosphere, the uniformity of pore-cells increases with the hydrogen pressure; while at a constant hydrogen pressure plus additional argon, the uniformity first increases with the argon pressure, then decreases. The influence of gas pressure on the uniformity is similar with that mentioned in section 'Nearest-neighbour distance distribution'. At a high hydrogen pressure and an appropriate argon pressure, pore-cells with relatively high degree of uniformity can be obtained.

Discussion

Characteristics of pore distribution

The second-order characteristics and the nearest-neighbour distance distribution of pores in lotus-type structure show that the pore distribution is short-range ordered. This type of distribution can be considered as a result of heavily disturbed regular distribution. In Gasar process many factors, such as the radial heat flux, the influence of inclusions

Table 2 The ratio Q & R for pore distribution on transverse cross-sections of lotus-type porous magnesium

Sample No.	1	2	3	4	5	6	7
Q	1.554	1.559	1.505	1.584	1.557	1.470	1.453
R	0.395	0.306	0.265	0.245	0.238	0.314	0.394

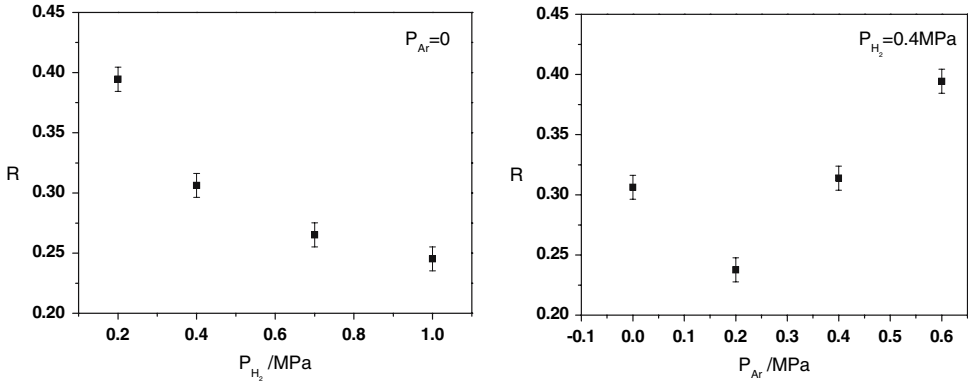

Fig. 7 Gas pressure versus regularity index *R*

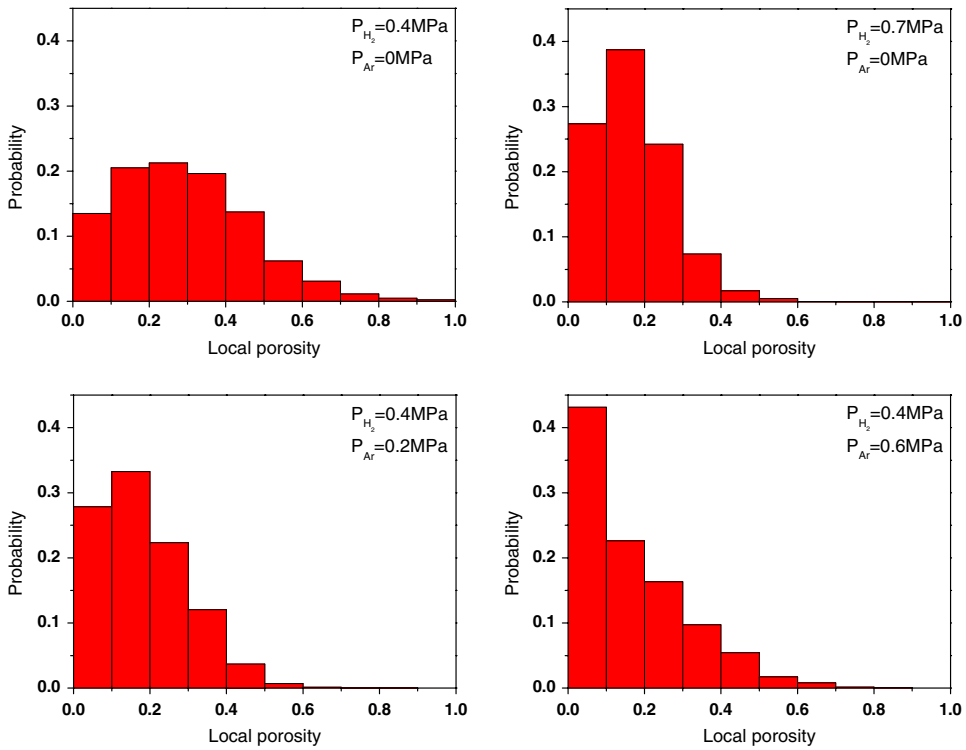

Fig. 8 Local porosity distribution of lotus-type porous magnesium

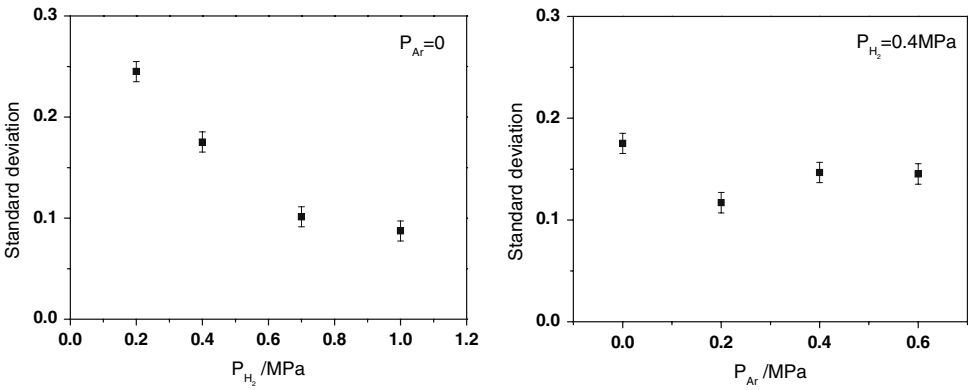

Fig. 9 Gas pressure versus standard deviation of the local porosity distribution

or wall cracks of the mould on bubble nucleation, the convection induced by escaped bubbles from the melt [16], etc., cause the solidification condition deviating from ideal steady-state. As a result, heavy disturbances make the actual pore distribution different from the ideal regular one corresponding to the ideal steady-state solidification, thus

the long-range order of the distribution disappears. On the other hand, the competition growth of pores results in the short-range regularity. The solute concentration gradient on the solidification front drives hydrogen diffusing into pores to keep cooperative growth of the gas and the solid phase. However, the solute diffusion, which controls the pore growth in the solidification [17], induces competition growth among pores. The pores without adequate solute diffusion will cease; new pores will form where the solute excessively concentrates [18]. Thus neighbouring pores can not distribute randomly but are constrained in an appropriate and relatively ordered arrangement by the concentration filed to keep steady growth.

Another characteristic of the pore distribution is the inhibition distance mentioned in section 'Second-order characteristics'. The pore pairs with distance less than the minimum distance never exist. This is due to that when two pores contact, the tips of them will coalesce to form one larger pore advancing to continue the growth [18], i.e. pores on the transverse cross-sections never grow with overlapping (however the shape of the transverse cross-section of pores where coalescence occurs may greatly different from circle).

Quantitative characterization indices

The microstructure of lotus-type porous metals can be quantitatively characterized by the statistics based parameters. This is very important in constructing relationships between processing parameters and material properties, which is essential in the selection of fabrication parameters, improvement of techniques and material designs. In this paper, the pore distribution in the lotus-type structure is quantitatively characterized by two parameters respectively. The ratio R mentioned in section 'Methods of measurement' is applied in quantitative characterization of regularity of the pore distribution; while the standard deviation of local porosity is found to be appropriate in characterizing the uniformity of pore-cells, because they are sensitive to the lotus-type structure fluctuation. Compared with the second-order intensity function and the pair correlation function, the two parameters are more adoptive as structural indices for quantitatively distinguishing specimens fabricated at various parameters.

Conclusions

1. The spatial distribution of pores in lotus-type porous metals is short-range ordered. In a range of about 2–3 times mean pore diameter, the pores are regularly distributed; while as the range increases, the pore distribution present notable randomness.
2. The ratio R deduced from the nearest-neighbour distance distribution of pore centroids and the standard deviation of local porosity can be applied in quantitative characterization of the lotus-type structure.

Acknowledgement Supported by National Key Basic Research and Development Program of China (No.2004CCA05100) and National Natural Science Foundation of China (No.50404002).

References

1. Shapovalov VI (1993) US. Patent No. 5,181,549
2. Nakajima H, Hyun SK, Ohashi K (2001) Colloid Surface A 179:209
3. Shapovalov VI (1994) Porous metals, MRS Bulletin, 24
4. Higuchi Y, Ohashi Y, Nakajima H (2005) In: Nakajima H, Kanetake N (ed) 4th International conference on porous metals and metal foaming technology, Kyoto, p 47
5. Park C, Nutt SR (1998) In: Porous and cellular materials for structural applications, materials research society symposium, vol 521. Materials Research Society, Pittsburgh PA, p 315
6. Boiko LV (2000) Mater Sci 36:506
7. Liu Y, Li YX, Zhang HW, Wan J (2005) Rare Metal Mat Eng 34:1128
8. Liu Y, Li YX, Wan J, Zhang HW (2005) Mat Sci Eng A 402:47
9. Nakajima H, Ikeda T, Hyun SK (2004) Adv Eng Mat 6:377
10. Pyrz R (1994) Compos Sci Technol 50:197
11. Schwarz H, Exner HE (1983) J Microsc 129:155
12. Wray PJ, Richmond O, Morrison HL (1983) Metallography 16:39
13. Everett RK, Chu JH (1993) J Compos Mater 27:1128
14. Spitzig WA, Kelly JF, Richmond O (1985) Metallography 18:235
15. Ohser J, Mücklich F (2000) In: Statistical analysis of microstructures in materials science. John Wiley & Sons, New York, p 270
16. Paradies CJ, Tobin A, Wolla J (1998) In: Porous and cellular materials for structural applications, materials research society symposium, vol 521. Materials Research Society: Pittsburgh PA, p 297
17. Liu Y, Li YX, Zhang HW, Wan J (2005) Acta Metallurgica Sinica 41:886
18. Shapovalov VI (1998) In: Porous and cellular materials for structural applications, materials research society symposium, vol 521. Materials Research Society: Pittsburgh PA, p 281